Dynamics of Bisphenol A Polycarbonate in the Glassy and Rubbery States As Studied by Neutron Scattering and Complementary Techniques

G. Floudas,*,† J. S. Higgins,‡ G. Meier,† F. Kremer,† and E. W. Fischer†

Max-Planck-Institut für Polymerforschung, P.O. Box 3148, 6500 Mainz, Germany, and Department of Chemical Engineering, Imperial College, London SW7 2BY, England

Received September 25, 1992; Revised Manuscript Received December 17, 1992

ABSTRACT: Quasielastic neutron scattering, dielectric spectroscopy, and mechanical relaxation have been employed to study the dynamics of Bisphenol A polycarbonate (BPA-PC) in the glassy and rubbery state. The neutron scattering measurements were made in the temperature range (ΔT) 296–586 K and over the Q-range 0.31–1.54 Å^{-1}, for the dielectric measurements in ΔT = 200–467 K and for the mechanical measurements in ΔT = 113–443 K. Using these techniques we obtain the dynamics associated with the primary (α-) relaxation and of the γ-relaxation in a frequency interval spanning 13 decades. The temperature dependence of the primary relaxation times conforms to the Vogel–Fulcher–Tammann equation, whereas the γ-relaxation times display an Arrhenius temperature dependence with an apparent activation energy of 10.8 kcal/mol. From the neutron scattering measurements, made in the gigahertz to terahertz frequency range, we obtain direct evidence that phenylene π-flips are not of paramount importance to the γ-relaxation. This is confirmed by the mechanical and neutron scattering measurements on the polycarbonate of 3,3′-dihydroxy-6,6′-dimethylbiphenyl (BPPC), which displays a similar γ-relaxation in which π-flips cannot participate.

Introduction

Glassy polycarbonate of Bisphenol A (BPA-PC) has been the subject of many investigations mainly because of its high impact strength (the ability to respond to sudden local strains) which is believed to arise from the ability to dissipate energy. Different mechanisms can lead to energy dissipation above and below the glass transition temperature T_g. Above T_g, energy is dissipated by the primary (α-)relaxation due to segmental motion, whereas below T_g the intermediate β-relaxation (a process which depends strongly on annealing), the "local" γ-relaxation which persist to low temperatures, and the δ-relaxation due to the methyl group rotation take over. Since β- and δ-relaxations are rather small in magnitude, the energy dissipation and consequently the high impact strength in glassy BPA-PC have been associated with the γ-relaxation.

In view of its important mechanical properties it is not surprising that the literature of BPA-PC is extensive, especially with regard to the γ-relaxation. A variety of NMR techniques have been employed,[1–9] together with mechanical relaxation,[10–12] dielectric spectroscopy,[13–16] and light scattering[17,18] in both bulk and dissolved polycarbonates. Theoretical models[19,20] have been applied to explain the dynamics in the glassy state and the conformational properties of BPA-PC and related compounds.[21–23] The structure factor of BPA-PC has been studied by neutron scattering[24,25] and wide-angle X-ray scattering.[26,27] Computer simulations[24,25] lead to the proposal of a banana-like shape of chains in the trans–trans conformation in the glassy polymer.

From the dynamic studies listed above two conflicting pictures emerged: NMR experiments demonstrated that rapid π-flips of the phenylene rings around their 1,4-axes, augmented by small-angle fluctuations, occur in glassy BPA-PC and give rise to the observed γ-relaxation. Mechanical and dielectric experiments, however, point out that the length scale of the γ-relaxation should involve more than a phenylene ring. Only such a motion could give rise to the pronounced mechanical low-temperature relaxation and the broad dielectric loss associated with the γ-relaxation. In fact, from recent dynamic mechanical experiments[12] it follows that more than one repeat unit is necessary for the γ-relaxation in BPA-PC. To reconcile the above pictures, two models have been proposed, one based on intramolecular cooperativity and one on intermolecular cooperativity. The first model[19] allows correlated conformational interchange between two neighboring carbonate units: an interchange between the trans–trans conformation of the first unit and the cis–trans conformation of the neighboring unit by rotation about one of the CO bonds in each of the two carbonate groups. During this exchange the phenylene rings are undergoing flips in association with the CO bond rotations, and one BPA-PC unit, between the two carbonates which interchange conformation, is translated and slightly reoriented. The second model[20] is based on geometrical considerations of the dense packing of chains in the glass and assumes intermolecular cooperative phenylene flips. The inherent mobility of isolated rings and the existence of independent wiggles are also allowed once the lattice distorts.

The purpose of the present study is to shed some light on the relaxation behavior of BPA-PC by combining the information from dielectric spectroscopy (DS) and mechanical relaxation (MR) at low frequencies with neutron scattering (NS) measurements at high frequencies on the same sample. The advantage of using neutron scattering in comparison to conventional techniques is that we can obtain simultaneously information on the geometry of the motion from the Q-dependence. This latter information is not accessible in other experiments. Furthermore, we employ NS and MR on the polycarbonate of 3,3′-dihydroxy-6,6′-dimethylbiphenyl (BPPC), a molecule with phenylene rings that cannot flip, and we compare the dynamics of this polymer with BPA-PC.

Experimental Section

The weight- and number-average molecular weights of the polycarbonate of Bisphenol A (Bayer) were M_w = 30 200 and M_n = 10 400, respectively, as determined by gel permeation chromatography (GPC) calibrated by a polycarbonate standard. The glass transition temperature was 420 K as determined by differential scanning calorimetry (DSC) at a heating rate of 10 K/min. Thin films (thickness ~0.15 mm) were prepared by

* Author to whom correspondence is addressed.
† Max-Planck Institut für Polymerforschung.
‡ Imperial College.

0024-9297/93/2226-1676$04.00/0

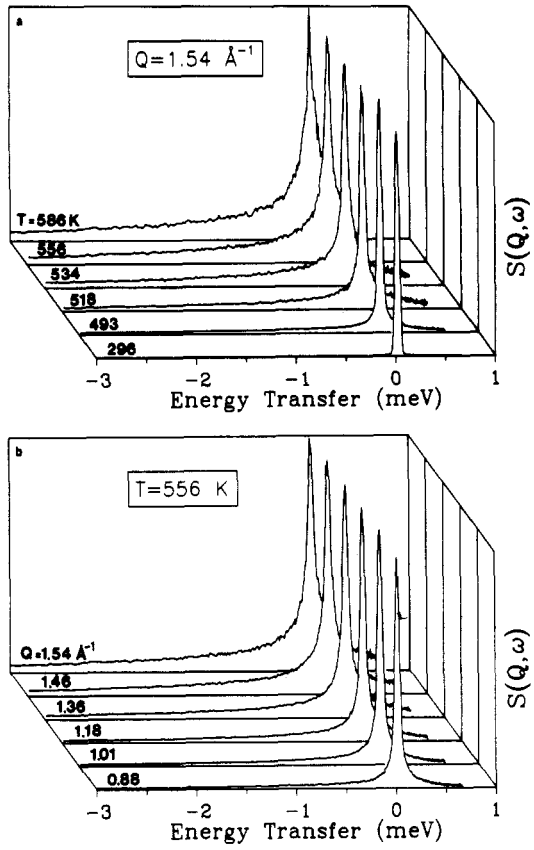

Figure 1. Quasielastic scattering spectra of BPA-PC (a) as a function of temperature at $Q = 1.54$ Å^{-1} and (b) as a function of Q at $T = 556$ K. The spectrum at $T = 296$ K corresponds to the spectrometer resolution function (triangular) which was used in the convolution procedure.

casting CH_2Cl_2 solutions of BPA-PC on glass plates and used in the NS and DS experiments. The films were dried under vacuum at 330 K for 7 days prior to the experiment. The polycarbonate of 3,3'-dihydroxy-6,6'-dimethylbiphenyl (BPPC)[28] had a molecular weight of $M_w = 98\,000$ and a T_g of 428 K which is only 8 K higher than that of BPA-PC. A selectively deuterated sample—on the methyl groups—and a completely hydrogenous sample were used in the neutron scattering and dynamic mechanical experiments, respectively.

The neutron scattering measurements on the BPA-PC sample were carried out on the time-of-flight spectrometer (MIBEMOL) at the reactor Orphée at the Laboratoire Léon Brillouin, CE-Saclay, France. The incident neutron wavelength was 7.5 Å, giving scattering vectors in the range 0.31–1.54 Å^{-1} with an energy resolution of 50 μeV (full width at half-height, fwhh). The BPA-PC film was contained in a flat Al container which was mounted on a liquid-helium cryostat at 30° to the incident neutron beam. Measurements were made in the $\Delta T = 296$–586 K range. Typical spectra as a function of T and Q are shown in Figure 1. The spectrum at the lowest temperature (296 K) in Figure 1a corresponds to the spectrometer resolution function. Starting from this temperature, we monitored the neutron intensity scattered at zero energy transfer (elastic-window T-scan), giving $S(Q,\omega\approx0)$. This quantity was measured for different Q-values as a function of T. Values normalized to the extrapolated intensity at 0 K are shown in Figure 2. The elastic-window T-scan shows distinct changes which are discussed in the next section. Long-time measurements were performed at selected temperatures: 518, 534, 556, and 586 K with a stability better than 1 K. The T- and Q-dependences of the quasielastic broadening in these measurements are discussed in the last section. The neutron scattering measurements on BPPC were made with the back-scattering spectrometer IN13 at the Institute Laue-Langevin (ILL), Grenoble, France. The incident neutron wavelength was 2.23 Å and the Q-range from 0.3 to 5 Å^{-1} with an energy resolution of 8 μeV (fwhh). The energy range covered was from −0.1 to 0.2 meV. The elastic-window T-scan for BPPC is shown in Figure 3 in the $\Delta T = 5$–475 K range. Longer measurements were made at 468, 500, and 520 K.

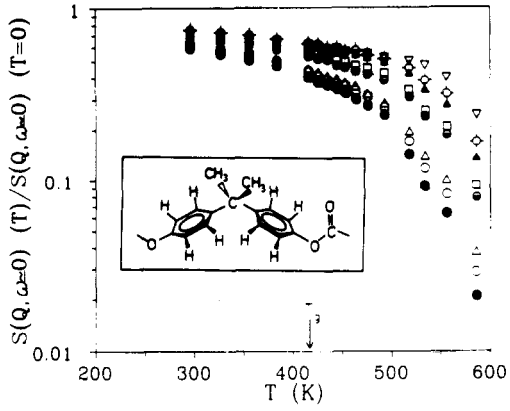

Figure 2. Temperature dependence of the incoherent dynamic structure factor $S(Q,\omega\approx0)$ (elastic-window T-scan) for BPA-PC, normalized to its value at $T = 0$ K and plotted for selected Q-values: (▽) $Q = 0.31$ Å^{-1}, (◇) $Q = 0.57$ Å^{-1}, (▲) $Q = 0.68$ Å^{-1}, (□) $Q = 0.88$ Å^{-1}, (⊖) $Q = 1.01$ Å^{-1}, (△) $Q = 1.36$ Å^{-1}, (○) $Q = 1.46$ Å^{-1}, (●) $Q = 1.54$ Å^{-1}. Notice the decrease of the elastic intensity beyond the Debye–Waller factor starting at $T \leq T_g$ which depends strongly on Q and T and which gives rise to the observed quasielastic broadening. The repeat unit of BPA-PC is shown in the inset.

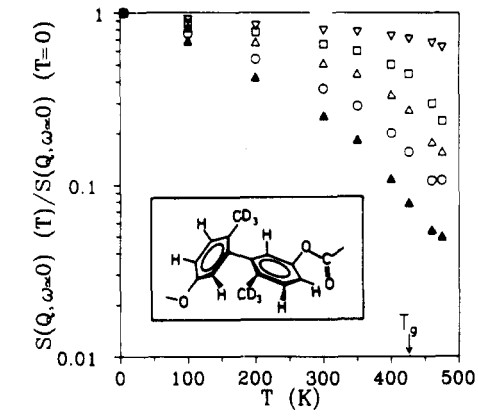

Figure 3. Temperature dependence of the incoherent dynamic structure factor $S(Q,\omega\approx0)$ for BPPC, normalized to its value at the lowest measurement temperature ($T = 5$ K) and plotted for selected Q-values: (▽) $Q = 0.56$ Å^{-1}, (□) $Q = 1.59$ Å^{-1}, (△) $Q = 2.56$ Å^{-1}, (○) $Q = 3.44$ Å^{-1}, (▲) $Q = 4.26$ Å^{-1}. The inset gives the repeat unit of BPPC.

The dielectric measurements on BPA-PC were carried out in the frequency range from 10^{-1} to 10^6 Hz with a frequency response analyzer (Solartron Schlumberger 1254), in the $\Delta T = 200$–467 K range. Gold electrodes were evaporated on the surfaces of the BPA-PC film, and the sample cell was mounted in a custom-made cryostat. Temperature calibration was accomplished by a jet of temperature-controlled nitrogen gas. The temperature stability during the measurements was better than ± 0.5 K. Details of the experimental setup are given in ref 29. The real (ϵ') and imaginary parts (ϵ'') of the complex permittivity $\epsilon^*(\omega)$ ($=\epsilon'(\omega) - i\epsilon''(\omega)$) are plotted in Figure 4 for the low-T γ-relaxation as a function of frequency.

The dynamic mechanical measurements were carried out with a Rheometrics RMS 800 spectrometer which was used in the shear mode. The storage modulus G' and loss modulus G'' were measured in the $\Delta T = 113$–443 K range and for 10 frequencies between 0.1 and 100 rad/s. Typical dynamic mechanical G' and G'' curves as a function of T at 15.9 Hz are shown in Figure 5. For BPPC a measurement at one frequency (10 Hz) was made in the tensile mode with a DMTA spectrometer.

Data Analysis

The dielectric relaxation data (Figure 4) are very broad and asymmetric in shape. The four-parameter empirical

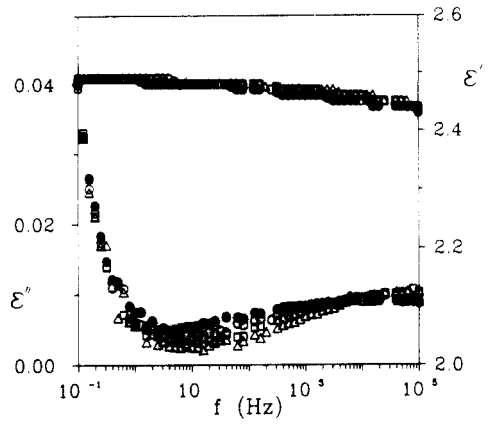

Figure 4. Real (ϵ') and imaginary parts (ϵ'') of the complex permittivity as a function of frequency plotted for different temperatures: (●) T = 200.6 K, (○) T = 209 K, (□) T = 218 K, (△) T = 225.7 K, corresponding to the γ-relaxation of BPA-PC.

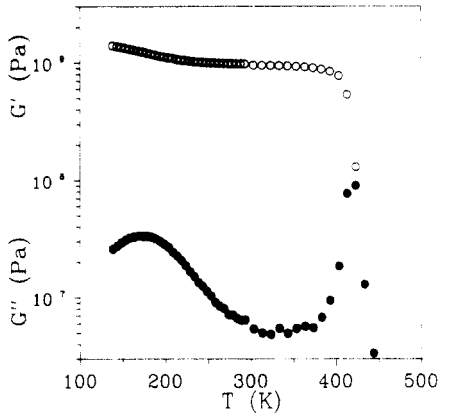

Figure 5. Storage G' and loss G'' moduli at 15.9 Hz as a function of temperature for BPA-PC.

equation of Havriliak–Negami (HN)[30]

$$\epsilon^*(\omega) = \epsilon_\infty + \frac{\epsilon_0 - \epsilon_\infty}{[1 + (i\omega\tau_{HN})^\alpha]^\gamma} \qquad (0 < \alpha, \gamma \leq 1) \qquad (1)$$

was used to fit the relaxation part of the α- and γ-relaxations. In eq 1, ϵ_0 and ϵ_∞ are respectively the low- and high-frequency values of the real part of the dielectric permittivity for the process under investigation and τ_{HN} is the characteristic relaxation time. Two parameters (α and γ) are used to characterize the symmetrical and asymmetrical broadening of the distribution of relaxation times, respectively. Figure 6 shows a fit to the experimental data for the γ-relaxation. The steep rise at low frequencies (Figures 4 and 6) is caused by the electrical conductivity within the sample, which has been fitted according to $\epsilon'' \sim (\sigma_0/\epsilon_0)\omega^{s-1}$ where σ_0 and s ($0 \leq s \leq 1$) are fitting parameters and ϵ_0 denotes the permittivity in vacuo. The shape parameters (α, γ) were found to be temperature dependent for both the α- and γ-relaxations, but this dependence is more pronounced in the latter: the parameters (α, γ) increased from (0.27, 0.37) at 200 K to (0.36, 0.48) at 226 K. This indicates that the distribution of relaxation times narrows with increasing T. This finding is in agreement with earlier DS studies on BPA-PC.[13,14]

With incoherent neutron scattering the dynamic structure factor

$$S_{inc}(Q,\omega) \sim \int \exp(-i\omega t)C(t)\, dt \qquad (2)$$

is measured, where $C(t)$ is the single-particle density

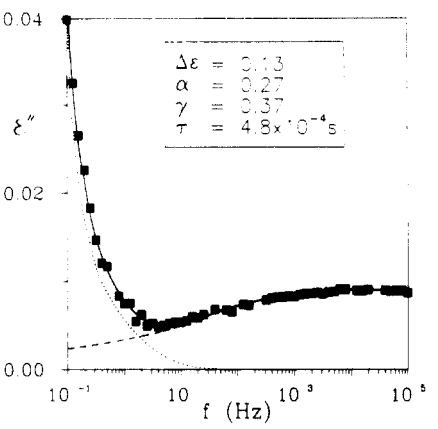

Figure 6. Fit to the dielectric loss curve at 200.6 K using the HN equation (eq 1). The steep rise at low frequencies (dotted line) is due to the conductivity contribution, whereas the relaxation part is denoted by a dashed line. The solid line is the superposition of the conductivity and relaxation contributions. The parameters of the HN equation are shown in the inset.

correlation function:

$$C(t) = \langle \exp[-i\mathbf{Q}\cdot(R_i(0) - R_i(t))] \rangle \qquad (3)$$

$R_i(0)$ and $R_i(t)$ are the positions of the ith nucleus at times 0 and t, and $\mathbf{Q}$ is the scattering vector defined in terms of the change in wave vector on scattering: $\mathbf{Q} = \mathbf{k}_i - \mathbf{k}_f$, where the subscripts i and f refer to the initial and scattered neutron beams, respectively. BPA-PC represents a strongly incoherent scatterer since it contains C, H, and O atoms, and the incoherent scattering cross section of H is very large compared to the incoherent and coherent cross sections of C and O (σ_{inc}^{total} = 1116 barn/monomer, σ_{coh}^{total} = 126 barn/monomer).

After the initial neutron counts were corrected for detector and monitor efficiency and for background scattering (taken separately with no sample in the beam), the time-of-flight (TOF) differential cross section $\partial^2\sigma/\partial\Omega\,\partial t$ was calculated, where t is the neutron TOF scattered into an element of solid angle $\partial\Omega$. From the measured TOF spectrum, the differential scattering cross section $\partial^2\sigma/\partial\Omega\,\partial E$ was calculated and the incoherent scattering law $S_{inc}(Q,\omega)$ was obtained from

$$S_{inc}(Q,\omega) = \frac{4\pi\hbar}{\sigma_{inc}}\frac{k_i}{k_f}\frac{\partial^2\sigma}{\partial\Omega\,\partial E} \qquad (4)$$

where σ_{inc} ($=4\pi[\langle b^2\rangle - \langle b\rangle^2]$) is the incoherent scattering cross section and b is the scattering length for hydrogen.

To fit the neutron scattering data of BPA-PC (Figure 1), we employed, to a first approximation, an elastic peak (delta function) plus a Lorentzian with a flat background. The elastic peak is due to motions slower than the resolution, whereas the broad Lorentzian peak is due to quasielastic broadening beyond the resolution function. However, such a fit produced strong and systematic deviation plots at all T and Q. It is apparent that another quasielastic component has to be included to fit the NS spectra. One might argue that a distribution of relaxation processes could describe the spectra. However, from previous NMR and from our DS and MR measurements we know that two distinct processes contribute to the relaxation spectra. Since one of these processes is due to the CH_3 rotation—which can be described by a single Lorentzian[15]—it is natural to use a second Lorentzian peak for the slower process provided that with this choice we can fit the data. Therefore, we have fitted our NS spectra with a delta function plus two Lorentzians on top of a flat

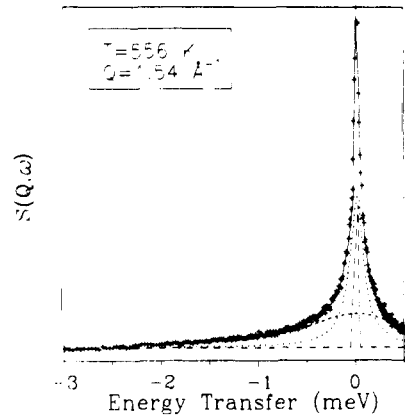

Figure 7. Quasielastic neutron scattering spectrum BPA-PC at $T = 556$ K and $Q = 1.54$ Å^{-1} showing the fit to (i) a delta function convoluted with the spectrometer resolution, (ii) a broad Lorentzian (hwhh, Γ_2), and (iii) a narrow Lorentzian (hwhh, Γ_1) on top of a flat background. The solid line is the result of the fit of eq 5 to the experimental data (+).

background:

$$S_{inc}(Q,\omega) = \frac{1}{\pi}\sum_{i=1}^{2} I_i(Q)\frac{\Gamma_i(Q)}{\Gamma_i^2(Q) + \omega^2} + B \qquad (5)$$

where I_i and Γ_i are the intensities and the corresponding hwhh. Using this model function we were able to fit the spectra at all T and Q. Figure 7 shows a fit to the spectrum at $T = 556$ K and $Q = 1.54$ Å^{-1} using eq 5. The neutron scattering data of BPPC were adequately fitted by a delta function plus one Lorentzian on top of a flat background, as expected, since no CH_3 group is present in this polymer.

Results and Discussion

1. Low-Frequency Side. Above T_g, the dielectric relaxation times conform to the Vogel–Fulcher–Tammann (VFT) equation:

$$\log \tau_{max} = \log \tau_0 + \frac{B}{T - T_0} \qquad (6)$$

with $\log \tau_0 = -14.8 \pm 0.5$ (τ in seconds), $B = 744 \pm 40$ K, and $T_0 = 373 \pm 5$ K. In eq 6, B is the apparent activation energy, T_0 is the "ideal" glass transition temperature located below the calorimetric T_g ($T_0 = T_g - c_2$, and c_2 is the WLF parameter), and τ_{max} is the time corresponding to the loss maximum (calculated from τ_{HN} and the parameters α and γ). Alternatively, the experimental relaxation times for the γ-relaxation conform to the Arrhenius equation:

$$\log \tau_{max} = \log \tau_0^* + \frac{E}{2.303RT} \qquad (7)$$

where $\log \tau_0^* = -16 \pm 0.5$ (τ in seconds) and $E = 11.9$ kcal/mol as obtained from the dynamic mechanical data alone. An interesting feature of this relaxation is the very broad distribution of relaxation times with very small HN parameters: i.e., $(\alpha, \gamma) = (0.27, 0.37)$ at $T = 200$ K. In fact, this low-T relaxation is broader than the α-relaxation at low frequencies. It is because of the broad distribution that this relaxation was earlier[14] described in terms of two distinct processes (γ_1 and γ_2). However, at higher T the distribution narrows and this is indicated by the higher (α, γ) values.

From the dielectric strength ($\Delta\epsilon$) of the α- and γ-relaxations—obtained from the fit to the experimental data using eq 1—we can calculate the relative number of dipoles activated in these relaxations from

$$\Delta\epsilon = \frac{4\pi N\mu^2}{9kT}\frac{\epsilon_0(\epsilon_\infty + 2)^2}{2\epsilon_0 + \epsilon_\infty} \qquad (8)$$

In eq 8, N denotes the number of monomeric units per unit volume and μ the dipole moment per monomer unit. In comparing the dielectric strength at the same frequency we obtain $(N_\mu^2)_\gamma = 0.25(N\mu^2)_\alpha = 0.2(N\mu^2)_{total}$. This indicates that 20% of the total dipoles are mobile in the glassy state, in agreement with an earlier estimation.[14] Alternatively, an estimation of the activated number of units in the γ-relaxation can be made by the recent "domain model".[31] According to this model, one repeat unit of BPA-PC consits of 3 conformers—a conformer being the smallest unit of rotation—and a typical domain size at T_g consists of approximately 7–10 conformers. For BPA-PC the size of the unit activated by the γ-relaxation was estimated to be 2–3 conformers which corresponds to approximately 30% of the units activated by the α-process close to T_g. On the other hand, from the dynamic mechanical measurements[12] on the alternating copolymer TMBPA-BPA it was shown that a cooperative motion of several monomer units is necessary in order to restore the low-T relaxations of the two homopolymers.

Therefore, the γ-relaxation in BPA-PC is manifested by the very broad distribution of relaxation times at low T, the exceptionally high preexponential factor in eq 7 and the relatively high number of activated chains. We discuss these findings together with the high-frequency-side data below.

2. High-Frequency Side. The NS spectra in Figure 1 display progressive quasielastic broadening with both T and Q. Quasielastic broadening is expected in view of the elastic-window T-scan (Figure 2) which shows that an initial elastic intensity reduction due to the normal Debye–Waller factor (DWF) ($\ln S(Q,\omega\approx 0) \sim -\langle r^2\rangle Q^2$, where $\langle r^2\rangle$ is the proton mean-square displacment due to vibrations) is followed by a more drastic drop at higher T. The lost elastic intensity reappears in the spectrum as quasielastic broadening. Furthermore, the distinct changes in $S(Q,\omega\approx 0)$ (Figure 2) as a function of T could imply either (i) two distinct motions giving rise to quasielastic broadening at $T > 500$ K or (ii) a change in the amplitude of a single motion. However, the presence of CH_3 groups in the repeat unit of BPA-PC is expected to give rise to the shortest relaxation time in this and other polymers,[32] and the extrapolation from the low-T γ-relaxation to higher T is also expected to contribute to some quasielastic broadening with relaxation times longer than for the methyl group motion. Therefore, implicit in the two-Lorentzian fit of eq 5 is the assumption of two distinct processes: the faster is due to the methyl group and the slower due to the γ-relaxation. The increase of the relative background in Figure 1a,b is only apparent. In fact, the background—in absolute units—decreases slightly with T and Q.

The line widths of the broader ("fast") and narrower ("slow") spectral components—obtained from a two-Lorentzian fit (Figure 7)—display a weak versus a stronger T- and Q-dependence within the T- and Q-ranges studied. The Q-dependence of the line widths at one temperature is shown in Figure 8, and the T-dependence at one Q-value is shown in Figure 9. It is evident from Figure 8 that, strictly speaking, neither of the two processes has a fixed center of mass. If the fast NS process was a mere CH_3 3-fold rotation and if the slow NS process was due to phenylene π-flips around their 1,4-axes, then both processes, having a fixed center of mass, should have been Q-independent, within the Q-range studied. Our results

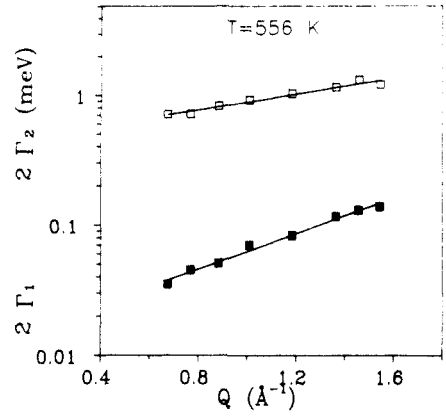

Figure 8. Full width at half-height (fwhh) $2\Gamma_1$ (■) and $2\Gamma_2$ (□) of the narrower and broader Lorentzians in eq 5, plotted as a function of Q, at $T = 556$ K. Solid lines are interpolations through the experimental points.

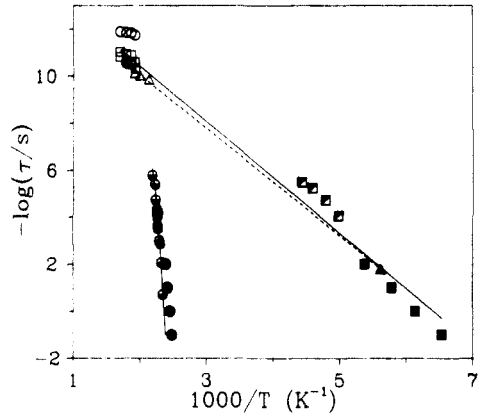

Figure 9. Transition map for BPA-PC and BPPC (triangles). The relaxation times for the (α- and γ-) processess of BPA-PC are obtained by mechanical relaxation (●, ■) and dielectric spectroscopy (◒, ◪), respectively. The "fast" neutron scattering process (○) attributed to the methyl group motion and the "slow" process (□) attributed to the γ-relaxation of BPA-PC are plotted for two Q-values (upper symbol, $Q = 1.3$ Å^{-1}; lower symbol, $Q = 0.8$ Å^{-1}). The relaxation time obtained from the Rayleigh-Brillouin experiment (●; ref 17) is also shown. Notice that this point is located in the extrapolation from the low-T γ-process. The solid line represents a fit to the γ-relaxation data of BPA-PC using eq 7. The plot includes the relaxation times for BPPC obtained from mechanical relaxation (△) and neutron scattering (▲) experiments. The dashed line is a fit to the γ-relaxation of BPPC.

with respect to Figure 8 demonstrate that the methyl groups perform some complex rotation, whereas the possibility of mere π-flips for the γ-relaxation is ruled out. However, judging from the relatively weak Q-dependence of the fast process, we can treat this motion—to a first approximation—as Q-independent.

In Figure 9, we compare the relaxation times from the slow NS process with the relaxation times obtained from MR and DS on the same sample. The fast NS process and the α-relaxation times are also included. Comparison of the slow Q-dependent NS times with the times from other experiments (MR, DS) where no Q is involved requires the use of a third axis to the usual two-dimensional Arrhenius plot to account for the Q-dependence.[33] However, in the logarithmic plot of Figure 9, differences between τ plotted for the different Q-values (Figure 8) are suppressed and can change the activation energy by only ~6%, which is within the experimental error. To demonstrate this, we plot the slow times at two Q-values in Figure 9. It is evident from Figure 9 that the origin of the slow NS process is the low-T γ-relaxation and the activation parameters from the NS, MR, and DS times are log $\tau_0^* = -15.1$ and $E = 10.8$ kcal/mol, only slightly different than the ones obtained from the MR data alone. It is also noteworthy that the Rayleigh-Brillouin data point,[17] obtained from the Brillouin line-width maximum, is located in the vicinity of the γ-relaxation rather than of the α-relaxation. This finding was discussed earlier[33] in the case of the glass-forming liquid di-2-ethylhexyl phthalate with the combination from light scattering, DS, and NS relaxation times.

The activation parameters for the γ-relaxation are in good agreement with earlier dynamic mechanical and dielectric studies on BPA-PC. Moreover, these parameters are obtained here on the same BPA-PC sample from a combination of DS, MR, and NS data spanning 13 decades of frequency. The distribution of relaxation times was estimated[5] previously in terms of the coupling model[5,34] from the dilute solution and bulk polymer activation energies with a value of $\beta \sim 0.2$ in the Kohlrausch-Williams-Watts representation. This is in agreement with the broad distribution obtained in the present DS study at low frequencies. Furthermore, we obtain the temperature dependence of this distribution and we suggest that at gigahertz frequencies the distribution has already collapsed into a single relaxation.

In the following, we compare the γ-relaxation in BPA-PC with that in BPPC. We would like to mention here again that in BPPC the two phenylene rings are bonded together, making a π-flip impossible. This was confirmed by pulsed ^{2}H NMR echo experiments at a ^{2}H Larmor frequency of about 55 MHz at $T = 310$ K and $T = 405$ K using a pulse sequence $(2\ \mu s)_x$–60 μs–$(2\ \mu s)_y$. We used 200 accumulations and adjusted the waiting time such that a fully relaxed spectrum would have resulted based on data for BPA-PC. The spectra, at both temperatures, looked like a rigid Pake spectrum, indicating the absence of phenyl flip motion. With respect to Figure 3, the elastic-window T-scan for BPPC displays a single continuous drop from the normal DWF. When compared at the same Q-value ($Q = 0.56$ Å^{-1}) with the corresponding scan for BPA-PC (Figure 2) at $T < 500$ K, the trend and absolute value of $S(Q,\omega\approx0)$ are similar. However, the underlying motion in BPA-PC and BPPC at $T < 500$ K is different, because a methyl group motion in the former is made "invisible" in the latter by selective deuteration. Therefore, the drop of the elastic intensity and the concomitant quasielastic broadening in BPPC reflects a "long-range" rather than a localized motion. The long-time measurements made at three temperatures above T_g clearly show—as expected—a quasielastic peak on top of a flat background which can be fitted by a single Lorentzian. The relaxation times obtained from this analysis are plotted in Figure 9. These data are combined with the MR data at 10 Hz. Parenthetically, the MR data of BPPC display a low-T relaxation similar to that for BPA-PC and only slightly shifted to lower T. The NS and MR times can be fitted according to eq 7, giving parameters: log $\tau_0^* = -14.6$ and $E = 10.4$ kcal/mol which are similar to the corresponding parameters for BPA-PC.

From the similar activation parameters for the γ-relaxation in BPPC and BPA-PC we can draw some conclusions about the molecular origin of this relaxation. First, the fact that the mechanical relaxation spectra of the two polymers are similar indicates that phenylene group π-flips—which admittedly exist in BPA-PC[1-9]—do not give rise to the mechanical γ-relaxation but can act as an indicator for it. The same can be said about the dielectric and more importantly about the slow NS process

at much higher frequencies. Second, if we assume that the γ-relaxation in BPA-PC and BPPC have the same molecular origin, then the two phenylene groups have to move cooperatively. In this motion the carbonate group is likely to participate. In fact, according to recent molecular orbital calculations,[22] the carbonate group in BPA-PC is relatively free of hindrance from the phenylene rings. As a result, the phenylene π-flips which were included in the model proposed by Jones[19] are not a necessity. This observation is consistent with the similar γ-relaxation times in BPA-PC and BPPC. This also compares with the results based on chemical shift tensors[35] and on dipolar tensors[36] which indicate only small-amplitude main-chain motion of both isopropylidene and carbonate sites. The question of whether or not and to what spatial extent the γ-relaxation involves intermolecular in addition to intramolecular cooperativity is more difficult to answer. However, we expect that some degree of intermolecular cooperativity must exist in view of the large shear waves in the Rayleigh–Brillouin spectrum.[17]

It is interesting at this point to obtain an estimate of the average hole size in glassy BPA-PC since we expect the range of the γ-relaxation to be of the same order. The γ-relaxation in BPA-PC is a result of density fluctuations in the glass. The density fluctuations can be measured by small-angle X-ray scattering (SAXS) through the scattered intensity at $Q \rightarrow 0$ ($Q = (4\pi/\lambda)\sin(\theta/2)$).[37] An estimate of the average hole size is then possible with the aid of a model[38] which relates the density fluctuations in the glass with the free (or hole) volume. The model assumes that (i) the location of the holes are entirely random in space so that the creation and annihilation of a hole is independent of the presence of nearby holes and that (ii) the size distribution among holes within the volume v is not influenced by the number of holes in v. Under these assumptions the intensity at zero Q, $I(0)$, is given by

$$I(0) = n^2\langle V\rangle_w \frac{f}{(1-f)^2} \qquad (9)$$

where n is the electron density, f is the fractional free volume, and $\langle V\rangle_w$ is the average volume of a hole. From the WLF parameters we obtain $f(T_g) = 0.027$ for BPA-PC, and from the values of $I(0)$ (=430 electrons^2 nm^{-3})[39] and specific volume (0.863 cm^3 g^{-1})[40] at T_g, we obtain a weight-average hole volume of (0.5 nm)^3 which corresponds to a hole diameter of approximately 6 Å.[41] It is worth mentioning that the rough estimate above is in agreement with the calculations based on a static atomistic model[23b] of dense glassy BPA-PC which revealed inhomogeneities in the form of "empty space" with a diameter of 3–5 Å.

The hole volume calculated above can accommodate less than a monomer unit. It is noteworthy that the model proposed by Jones[19] involves a cooperative motion ranging beyond a monomer unit (it involves three consecutive rings), whereas several monomer units were thought to contribute to the γ-relaxation from recent dynamic mechanical measurements.[12] However, it is difficult to rationalize how these motions can take place within the calculated hole size. Large-volume fluctuations are also excluded by pressure-dependent studies[42,43] which provide an activation volume smaller than the repeat unit volume of BPA-PC.

Concluding Remarks

We have studied the dynamics of Bisphenol A polycarbonate in the glassy and rubbery states with mechanical relaxation, dielectric spectroscopy, and, for the first time, incoherent neutron scattering over 13 decades of frequency. We obtain the dynamics associated with the primary (α-)relaxation and with the γ-relaxation which exhibit a Vogel–Fulcher–Tammann and an Arrhenius temperature dependence, respectively. The γ-relaxation is characterized by (i) an apparent activation energy of 10.8 kcal/mol, (ii) the very broad distribution of relaxation times, at low T, which depends strongly on T, (iii) the relatively high number of activated chains, and (iv) the Q-dependent quasielastic broadening at gigahertz frequencies.

In comparing the dynamics of BPA-PC with BPPC—where the two phenylene rings are bonded together making a π-flip impossible—we conclude that phenylene π-flips are not of paramount importance to the γ-relaxation. On the basis of the estimation of the hole size in glassy BPA-PC from density fluctuations, we propose that the length scale of this motion should involve not more than a monomer unit.

Acknowledgment. The authors are indebted to Prof. J.-P. Cotton and Dr. G. Coddens for beam time and help during the experiment on the spectrometer MIBEMOL (CE-Saclay, France). We are also indebted to Dr. W. Petry from the ILL, Grenoble, France, for providing beam time on the spectrometer IN13 (ILL) and to Dr. F. Fujara, University of Mainz, Mainz, FRG, for performing the ^{2}H NMR measurements on BPPC. Both colleagues further shared a good deal of time discussing the subject which helped to clarify the issue. We also thank Dr. T. Wagner (MPI-P) for the synthesis of BPPC and Dr. T. Pakula for the dynamic mechanical measurements.

References and Notes

(1) Schaefer, J.; Stejskal, E. O.; Buchdahl, R. *Macromolecules* **1977**, *10*, 384.
(2) Garfield, L. J. *J. Polym. Sci., Part C* **1970**, *30*, 551.
(3) Steger, T. R.; Schaefer, J.; Stejskal, E. O.; McKay, R. A. *Macromolecules* **1980**, *13*, 1127.
(4) O'Gara, J. F.; Desjardins, S. G.; Jones, A. A. *Macromolecules* **1981**, *14*, 64.
(5) Jones, A. A.; O'Gara, J. F.; Inglefield, P. T.; Bendler, J. T.; Yee, A. F.; Ngai, K. L. *Macromolecules* **1983**, *16*, 658.
(6) Fischer, E. W.; Hellmann, G. P.; Spiess, H. W.; Hörth, F.-J.; Ecarius, U.; Wehrle, M. *Macromol. Chem. Suppl.* **1985**, *12*, 189.
(7) Schmidt, C.; Kuhn, K. J.; Spiess, H. W. *Prog. Colloid Polym. Sci.* **1985**, *71*, 71.
(8) Wehrle, M.; Hellmann, G. P.; Spiess, H. W. *Colloid Polym. Sci.* **1987**, *265*, 815.
(9) Henrichs, P. M.; Nicely, V. A. *Macromolecules* **1991**, *24*, 2506.
(10) Yee, A. F.; Smith, S. A. *Macromolecules* **1981**, *14*, 54.
(11) Ngai, K. L.; Rendell, R. W.; Yee, A. F. *Macromolecules* **1988**, *21*, 3396.
(12) Jho, J. Y.; Yee, A. F. *Macromolecules* **1991**, *24*, 1905.
(13) Matsuoka, S.; Ishida, Y. *J. Polym. Sci., Part C* **1966**, *14*, 247.
(14) Watts, D. C.; Perry, E. P. *Polymer* **1978**, *19*, 248.
(15) Aoki, Y.; Britain, J. O. *J. Appl. Polym. Sci.* **1976**, *20*, 2879.
(16) Pochan, J. M.; Gibson, H. W.; Froix, M. F.; Hinman, D. F. *Macromolecules* **1978**, *11*, 163.
(17) Patterson, G. D. *J. Polym. Sci., Polym. Phys. Ed.* **1976**, *14*, 741.
(18) Foudas, G.; Lappas, A.; Fytas, G.; Meier, G. *Macromolecules* **1990**, *23*, 1747.
(19) Jones, A. A. *Macromolecules* **1985**, *18*, 902.
(20) Schaefer, J.; Stejskal, E. O.; Perchak, D.; Skolnick, J.; Yaris, R. *Macromolecules* **1985**, *18*, 368.
(21) Erman, B.; Marvin, D. C.; Irvine, P. A.; Flory, P. J. *Macromolecules* **1982**, *15*, 664.
(22) Sung, Y. J.; Chen, C. L.; Su, A. C. *Macromolecules* **1991**, *24*, 6123.
(23) (a) Hutnik, M.; Gentile, F. T.; Ludovice, P. J.; Suter, U. W.; Argon, A. S. *Macromolecules* **1991**, *24*, 5962. (b) Hutnik, M.; Argon, A. S.; Suter, U. W. *Macromolecules* **1991**, *24*, 5970.
(24) Červinka, L.; Fischer, E. W.; Hahn, K.; Jiang, B.-Z.; Hellmann, G. P.; Kuhn, K.-J. *Polymer* **1987**, *28*, 1287.
(25) Červinka, L.; Fischer, E. W.; Dettenmaier, M. *Polymer* **1991**, *32*, 12.
(26) Mitchell, G. R.; Windle, A. H. *Colloid Polym. Sci.* **1985**, *263*, 280.

(27) Schubach, H. R.; Heise, B. *Colloid Polym. Sci.* **1986**, *264*, 335.
(28) The synthesis and characterization of BPPC is reported by: Hörth, F.-J. Ph.D. Thesis, University of Mainz, Mainz, FRG, 1986.
(29) Kremer, F.; Boese, D.; Meier, G.; Fischer, E. W. *Prog. Colloid Polym. Sci.* **1989**, *80*, 129.
(30) Havriliak, S.; Negami, S. *Polymer* **1967**, *8*, 101.
(31) Matsuoka, S.; Quan, X. *Macromolecules* **1991**, *24*, 2770.
(32) Floudas, G.; Higgins, J. S. *Polymer* **1992**, *33*, 4121.
(33) Floudas, G.; Higgins, J. S.; Fytas, G. *J. Chem. Phys.* **1992**, *96*, 7672.
(34) For a review, see: Ngai, K. L.; Rendell, R. W.; Rajagopal, A. K.; Teitler, S. *J. Chem. Phys.* **1988**, *88*, 5086.
(35) Henrichs, P. M.; Linder, M.; Hewitt, J. M.; Massa, D.; Isaacson, H. V. *Macromolecules* **1984**, *17*, 2412.
(36) Poliks, M. D.; Gullion, T.; Schaefer, J. *Macromolecules* **1990**, *23*, 2678.
(37) See, for example: Wendorff, J. H.; Fischer, E. W. *Kolloid Z. Z. Polym.* **1973**, *251*, 876.
(38) Curo, J. J.; Roe, R.-J. *Polymer* **1984**, *25*, 1424.
(39) Floudas, G.; Pakula, T.; Stamm, M.; Fischer, E. W. *Macromolecules*, in press.
(40) Zoller, P. *J. Polym. Sci., Polym. Phys. Ed.* **1982**, *20*, 1453.
(41) An estimation of the hole size in BPA-PC based on the positronium annihilation and ultrasonic velocity data gives a smaller hole diameter (~3.4 Å). Malhotra, B. D.; Pethrick, R. A. *Eur. Polym. J.* **1983**, *19*, 457; *Polym. Commun.* **1983**, *24*, 165.
(42) Walton, J. H.; Lizak, M. J.; Conradi, M. S.; Gullion, T.; Schaefer, J. *Macromolecules* **1990**, *23*, 416.
(43) Hansen, M. T.; Kulik, A. S.; Prins, K. O.; Spiess H. W. *Polym. Commun.* **1992**, *33*, 2231.